

# Comparison of inclusive $K^+$ production in proton-proton and proton-neutron collisions

Yu. Valdau,<sup>1,2,\*</sup> V. Koptev,<sup>1</sup> S. Barsov,<sup>1</sup> M. Büscher,<sup>2</sup> A. Dzyuba,<sup>1</sup> M. Hartmann,<sup>2</sup>  
A. Kacharava,<sup>2</sup> I. Keshelashvili,<sup>3</sup> A. Khokaz,<sup>4</sup> S. Mikirtychians,<sup>1,2</sup> M. Nekipelov,<sup>2</sup>  
A. Polyanskiy,<sup>2,5</sup> F. Rathmann,<sup>2</sup> H. Ströher,<sup>2</sup> Yu. N. Uzikov,<sup>6</sup> and C. Wilkin<sup>7,†</sup>

<sup>1</sup>High Energy Physics Department, Petersburg Nuclear Physics Institute, RU-188350 Gatchina, Russia

<sup>2</sup>Institut für Kernphysik and Jülich Centre for Hadron Physics,  
Forschungszentrum Jülich, D-52425 Jülich, Germany

<sup>3</sup>Department of Physics, University of Basel, Klingelbergstrasse 82, CH-4056, Basel, Switzerland

<sup>4</sup>Institut für Kernphysik, Universität Münster, D-48149 Münster, Germany

<sup>5</sup>Institute for Theoretical and Experimental Physics, RU-117218 Moscow, Russia

<sup>6</sup>Laboratory of Nuclear Problems, JINR, RU-141980 Dubna, Russia

<sup>7</sup>Physics and Astronomy Department, UCL, London, WC1E 6BT, United Kingdom

(Dated: February 18, 2022)

The momentum spectra of  $K^+$  produced at small angles in proton-proton and proton-deuteron collisions have been measured at four beam energies, 1.826, 1.920, 2.020, and 2.650 GeV, using the ANKE spectrometer at COSY-Jülich. After making corrections for Fermi motion and shadowing, the data indicate that  $K^+$  production near threshold is stronger in  $pp$ - than in  $pn$ -induced reactions. However, most of this difference could be made up by the unobserved  $K^0$  production in the  $pn$  case.

PACS numbers: 13.75.-n, 14.40.Df, 25.40.Ve

## I. INTRODUCTION

A large series of results on  $K^+$  production in proton-nucleus [1] and nucleus-nucleus collisions [2] has been compiled in the low energy region. Although different nuclear models have been used to describe these data [3, 4], the crucial ingredients in any theoretical interpretation must be the cross sections for strangeness production in proton-proton and proton-neutron reactions. Parameterizations of the existing experimental data, or calculations within a meson-exchange model [5], have generally been employed for this purpose [6].

There are three strangeness-conserving  $K^+$  production channels that are open in  $pp$  collisions close to threshold. The one that has been most widely investigated is  $pp \rightarrow K^+p\Lambda$ , for which data on the total cross section, Dalitz plots, and angular spectra have been published [7–16]. In the  $pp \rightarrow K^+p\Sigma^0$  case, values of the total cross sections [9, 10] and angular distributions [16] are available. Parameterizations [17] of the energy dependence of the total cross sections for  $\Lambda$  and  $\Sigma^0$  production are shown in Fig. 1 alongside the available experimental data. Measurements also exist of the  $pp \rightarrow K^+n\Sigma^+$  total cross section [14, 15, 18] and studies of the  $pp \rightarrow K^0p\Sigma^+$  channel have been undertaken [19, 20].

In contrast, very little is known experimentally about  $K^+$  production in proton-neutron collisions. There are a few  $np \rightarrow K^+p\Sigma^-$  data points obtained with a neutron beam [21], though only at 3.4 GeV and above. There seem to be no measurements of the  $pn \rightarrow K^+n\Lambda$  or

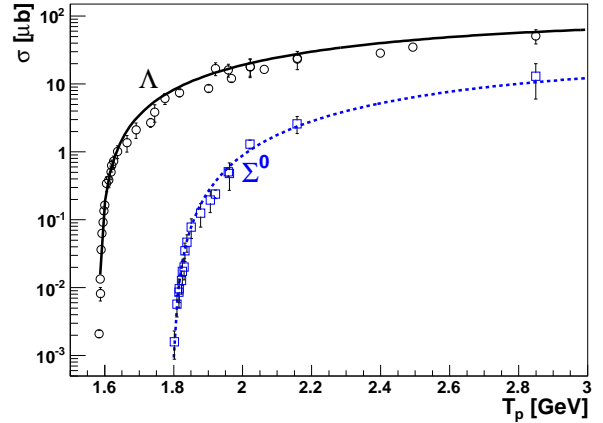


FIG. 1: (Color online) Compilation of total cross sections for the  $pp \rightarrow K^+p\Lambda$  (black circles), and  $pp \rightarrow K^+p\Sigma^0$  (blue squares) reactions. The experimental data are taken from Refs. [7–15]. Parametrizations of experimental data for  $\Lambda$  and  $\Sigma^0$  production from Ref. [17] are presented by solid black and dashed blue lines, respectively.

$pn \rightarrow K^+n\Sigma^0$  reaction channels recorded in the literature. However, some data on  $pn \rightarrow K^+n\Sigma^-$  have been obtained using the COSY-ANKE spectrometer [22] and results on the  $pn \rightarrow K^+n\Lambda$  reaction close to threshold should eventually be available from this facility [23] as will  $pn \rightarrow K^0p\Lambda$  from the COSY-TOF spectrometer [24].

Several attempts have been made to deduce the ratio of  $K^+$  production in  $pp$  and  $pn$  collisions,  $\sigma_{pn}^{K^+}/\sigma_{pp}^{K^+}$ , by analyzing data obtained using different nuclear targets and beams. The rather inconclusive value of  $\sigma_{pn}^{K^+}/\sigma_{pp}^{K^+} = 5 \pm 7.5$  was obtained with a 3 GeV proton beam incident

\*Electronic address: y.valdau@fz-juelich.de

†Electronic address: cw@hep.ucl.ac.uk

on a range of nuclei [25]. The comparison of the  $K^+$  production rate on a NaF target with proton and deuteron beams of energy 2.1 GeV per nucleon yielded a ratio  $\sigma(d\text{NaF} \rightarrow KX)/\sigma(p\text{NaF} \rightarrow KX) = 1.3 \pm 0.2$ , from which it was concluded that  $\sigma_{pn}^{K^+}/\sigma_{pp}^{K^+} < 1$  [26]. The ratio of double-differential  $K^+$  production cross sections measured with carbon and hydrogen targets at 2.5 GeV was interpreted as evidence that  $\sigma_{pn}^{K^+}/\sigma_{pp}^{K^+} \approx 1$  [27]. However, an analysis of the double-differential cross section for  $K^+$  production with a 2.02 GeV proton beam incident on a deuterium target gave the much larger but very model-dependent estimate of  $\sigma_{pn}^{K^+}/\sigma_{pp}^{K^+} \approx 3 - 4$  [1].

In the absence of reliable experimental proton-neutron data, it is interesting to see if theory can offer any guidance. The models that have been used are mainly of the one-meson-exchange variety, though these are very uncertain even for the  $pp \rightarrow K^+p\Lambda$  reaction since there is no consensus as to which exchanges need to be included. The results of the COSY-TOF collaboration, and in particular the evidence for the excitation of  $N^*$  isobars, suggest the dominance of non-strange meson exchange [28]. On the other hand, measurements of the spin-transfer parameter  $D_{NN}$  have been interpreted as indicating that strange meson exchange is the more important [29]. The picture is even less clear in the  $pn$  case, with theoretical estimates of  $\sigma(pn \rightarrow K^+n\Lambda)/\sigma(pp \rightarrow K^+p\Lambda)$  ranging from 0.25 to 5 [30], or around 2 [5] or 3 [31], depending upon the assumptions made.

The situation can only be clarified by further experimental work. This is reported here in the form of inclusive  $K^+$  momentum spectra measured on hydrogen and deuterium targets at four proton beam energies. The comparison of the results on the two targets allows one to make estimates of  $\sigma_{pn}^{K^+}/\sigma_{pp}^{K^+}$ . The experimental setup used to carry out the measurements is described in Sec. II. The results for the two targets are presented in Sec. III, where it is clearly seen that the small angle production rates from deuterium fall well below a factor of two times those on hydrogen.

The  $pp$  data are modeled in Sec. IV in terms of contributions from the  $pp \rightarrow K^+p\Lambda$  and  $pp \rightarrow K^+N\Sigma$  channels, with the normalizations chosen to fit the known total cross sections. Such an approach is very successful at the three lower energies but fails badly at 2.65 GeV when heavier hyperons and extra pions can be produced. In order to clarify the effects of the kinematics, the cross sections were smeared over the Fermi motion in the deuteron, though the resultant changes were fairly minor. Taking into account a small shadowing correction, it is seen in Sec. V that  $K^+n\Lambda$  production on the neutron is about half of that for  $K^+p\Lambda$  on the proton. However, since half the strength in the  $pn$  case should emerge in the  $K^0p\Lambda$  channel, our result is consistent with strangeness production near threshold being of similar size for both isospin  $I = 1$  and  $I = 0$ . Our conclusions and outlook for further work are reported in Sec. VI.

## II. EXPERIMENTAL METHOD

The experiments were carried out at the Cooler-Synchrotron COSY-Jülich [32] using unpolarized proton beams incident on hydrogen and deuterium cluster-jet targets [33]. The resulting reaction products were detected in the ANKE magnetic spectrometer [34], which is situated in a chicane inside the COSY ring. The spectrometer uses three dipole magnets.  $D1$  and  $D3$  divert the circulating beam onto the ANKE target and back into the COSY ring, respectively, while  $D2$  is the analyzing magnet. All data with the hydrogen target and those with deuterium at  $T_p = 2.650$  GeV were collected using the same magnetic field in  $D2$  ( $B_{\text{max}} = 1.568$  T). Deuterium data at 1.826, 1.920 and 2.020 GeV were taken using  $B_{\text{max}} = 1.445, 1.505$  and  $1.570$  T, respectively.

The layout of the relevant elements of the ANKE detector systems is sketched in Fig. 2. Only information provided by the positive detector (Pd), forward detector (Fd) and a prototype of the silicon tracking telescope (STT) was used in the present analysis. The Pd detector system consists of start and stop counters for time-of-flight measurements, two multiwire proportional chambers for momentum reconstruction and background suppression, and range telescopes for  $K^+$  identification.

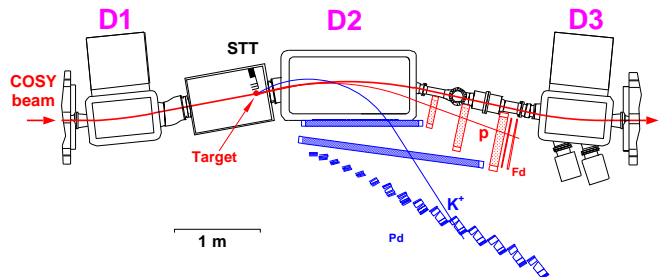


FIG. 2: (Color online) Sketch of the relevant parts of the ANKE detector system, showing the positions of the two bending magnets  $D1$  and  $D3$  and the target placed before the analyzing magnet  $D2$ . Only information obtained from the forward (Fd), positive side (Pd) detectors, and the Silicon Tracking Telescope (STT) was used in this experiment. Typical trajectories, leading to the measurement of protons and  $K^+$ , are also shown.

Fifteen range telescopes were placed in the focal plane of the  $D2$  magnet. Each of them consists of a stop counter, two copper degraders, a counter for measuring the energy loss ( $\Delta E$  counter) and one for detecting the  $K^+$  decay products (veto counter). The thickness of the first degrader was chosen such that the kaon deposits maximal energy in the  $\Delta E$  counter and stops either at its edge or in the second degrader. Measurements of the time difference between the  $K^+$  in the stop counter and its decay products in the veto counter provide a clear  $K^+$  identification even if the background from pions and protons is  $10^6$  times higher [35]. The efficiency of each range telescope, which was between 10% and 30% depending

upon the particular telescope, the parameters of the cuts, and the trigger conditions, were determined from the experimental data. The overall uncertainty from telescope to telescope arising from this efficiency correction was estimated with an accuracy of  $\approx 15\%$  for the  $pd$  data and the  $pp$  at 2.65 GeV, and  $\approx 10\%$  for the other  $pp$  runs. Full details of  $K^+$  identification using the ANKE range telescopes can be found in Ref. [35].

The cross section normalizations were established from the information supplied by the Fd detector system, as described in Ref. [36]. The Fd consists of three multiwire chambers and a hodoscope of scintillators. In the hydrogen-target experiments, and for deuterium at 2.650 GeV, the first multiwire proportional chamber was replaced by a drift chamber. For the hydrogen experiments, a dedicated prescaled trigger was used to monitor the  $pp$  elastic scattering rate throughout the experimental runs. Elastic scattering events were identified in the angular range  $6.0^\circ$ – $9.0^\circ$  in the forward detector using the missing-mass technique. The luminosity was then evaluated on the basis of the known  $pp$  differential cross sections with an overall normalization error of 7% [15].

A similar method was employed to normalize the 2.650 GeV  $pd$  data. The prescaled rate for the production of fast protons from proton-deuteron collisions was continuously monitored in the forward detector over the angular range  $7.0^\circ$ – $9.0^\circ$ . Because it was not possible to distinguish between elastic scattering and deuteron break-up events, the experimental count rate was converted into luminosity estimates through calculations carried out within the Glauber-Sitenko theory [37]. The associated overall normalization error should not exceed 15% [38].

The coincidence of signals from the silicon tracking telescope and forward detector was used to measure  $pd$  elastic scattering at 1.826, 1.920 and 2.020 GeV. The STT consists of three silicon detectors placed in ultra-high vacuum, with the first layer being 5 cm from the beam-target interaction point [39]. The identification of the deuteron in the STT, together with a proton in the Fd, allows one to select unambiguously elastic  $pd \rightarrow pd$  events. However, uncertainties in the evaluation of the acceptance *etc.* means that the overall absolute normalization error was 20%, though the relative error between different beam energies was at most 5% [40].

### III. EXPERIMENTAL RESULTS

The double-differential cross section for  $K^+$  production in each momentum bin  $\Delta p$  is evaluated from

$$d\sigma^{K^+} \equiv \frac{d^2\sigma_{K^+}}{d\Omega dp}(T_p) = \frac{N_{K^+}}{\Delta p \Delta\Omega} \frac{1}{L^{\text{tot}} \epsilon_{K^+}}, \quad (1)$$

where  $N_{K^+}$  is the number of  $K^+$  detected in a solid angle  $\Delta\Omega$  and  $L^{\text{tot}}$  is the integrated luminosity. The efficiency of  $K^+$  identification,  $\epsilon_{K^+}$ , is estimated from

$$\epsilon_{K^+} = \epsilon^{\text{tel}} \times \epsilon^{\text{scint}} \times \epsilon^{\text{MWPC}} \times \epsilon^{\text{acc}}. \quad (2)$$

The scintillator ( $\epsilon^{\text{scint}}$ ) and MWPC ( $\epsilon^{\text{MWPC}}$ ) efficiencies are determined from the experimental data. The kaon acceptance, including corrections for decay in flight, ( $\epsilon^{\text{acc}}$ ) is determined using simulations. The range-telescope efficiency  $\epsilon^{\text{tel}}$ , whose value is extracted from calibration data on  $K^+p$  coincidences, represents the main systematic uncertainty in the cross section evaluation [15].

The laboratory double-differential cross section for  $K^+$  production on hydrogen (open symbols) and deuterium (closed symbols) are presented at the four different beam energies in Fig. 3 as functions of the kaon momentum. The cross sections represent averages over  $K^+$  laboratory production angles up to  $4^\circ$ ; the measured values are also collected in Table I.

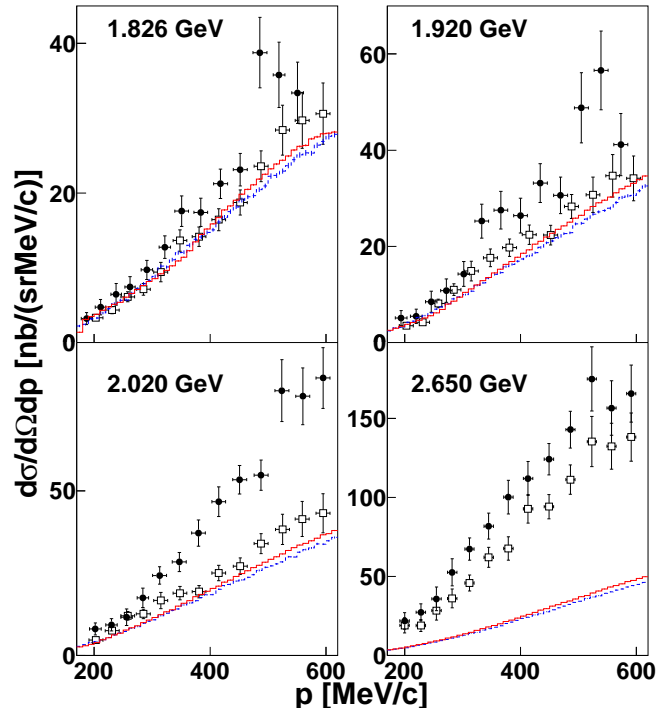


FIG. 3: (Color online) Momentum spectra of  $K^+$  produced in  $pp$  (open circles) and  $pd$  (closed circles) collisions at 1.826, 1.920, 2.020, and 2.650 GeV. Only statistical errors are shown. The red lines represent the description of the  $pp$  data within the three-channel model whereas for the blue dashed ones the predictions have been smeared over the deuteron Fermi momentum and a correction made for the shadowing in the deuteron.

The double-differential cross sections for  $K^+$  production in  $pd$  and  $pp$  collisions, shown in Fig. 3, have rather similar shapes and their ratio depends only weakly on the kaon momentum. Because the  $pd$  data at the three lower energies were taken with different values of the  $D2$  magnetic field from those for  $pp$ , the associated momentum bins are slightly different. In these cases the ratio of the  $K^+$  production cross sections was evaluated by assuming a linear variation from one bin to the next. However, corrections for the data measured at 2.020 GeV are minimal.

$T_p = 1.826$ GeV		$T_p = 1.920$ GeV		$T_p = 2.020$ GeV		$T_p = 2.650$ GeV			
$p$	$d^2\sigma_{pd}^{K^+}/d\Omega dp$	$p$	$d^2\sigma_{pd}^{K^+}/d\Omega dp$	$p$	$d^2\sigma_{pd}^{K^+}/d\Omega dp$	$p$	$d^2\sigma_{pd}^{K^+}/d\Omega dp$	$d^2\sigma_{pp}^{K^+}/d\Omega dp$	$d\sigma_{pd}^{K^+}/d\sigma_{pp}^{K^+}$
MeV/c	nb/(sr MeV/c)	MeV/c	nb/(sr MeV/c)	MeV/c	nb/(sr MeV/c)	MeV/c	nb/(sr MeV/c)		
187 ± 9	3.2 ± 0.8	194 ± 10	5.1 ± 1.6	202 ± 10	8.1 ± 1.8	200 ± 8	21.9 ± 5.3	19.1 ± 4.7	1.14 ± 0.21
211 ± 9	4.7 ± 1.0	220 ± 10	5.5 ± 1.5	230 ± 10	9.3 ± 1.8	228 ± 8	27.4 ± 5.3	19.0 ± 3.8	1.34 ± 0.22
238 ± 9	6.5 ± 1.4	246 ± 10	8.5 ± 2.2	256 ± 10	11.6 ± 2.5	255 ± 8	35.9 ± 7.5	28.4 ± 6.0	1.38 ± 0.12
262 ± 9	7.4 ± 1.4	272 ± 10	10.8 ± 2.4	284 ± 10	17.5 ± 2.9	282 ± 8	52.6 ± 8.6	36.1 ± 6.0	1.39 ± 0.11
291 ± 10	9.7 ± 1.3	302 ± 10	14.3 ± 2.6	313 ± 12	24.3 ± 2.6	312 ± 8	67.4 ± 7.1	45.9 ± 5.0	1.48 ± 0.11
322 ± 10	12.8 ± 1.5	333 ± 12	25.3 ± 3.5	347 ± 12	28.4 ± 2.9	345 ± 8	81.8 ± 8.2	62.2 ± 6.3	1.35 ± 0.09
351 ± 12	17.6 ± 2.0	366 ± 12	27.5 ± 3.9	380 ± 12	37.2 ± 4.0	379 ± 8	100.2 ± 10.6	67.7 ± 7.3	1.52 ± 0.09
384 ± 12	17.4 ± 1.9	400 ± 12	26.4 ± 3.6	415 ± 12	46.7 ± 4.5	413 ± 8	112.0 ± 10.8	92.8 ± 9.0	1.32 ± 0.07
418 ± 12	21.2 ± 2.0	434 ± 12	33.2 ± 4.0	451 ± 12	53.4 ± 4.3	449 ± 8	124.2 ± 10.0	94.2 ± 7.7	1.40 ± 0.08
452 ± 12	23.1 ± 2.2	469 ± 12	30.6 ± 3.8	488 ± 12	54.7 ± 4.6	486 ± 8	142.9 ± 11.7	111.3 ± 9.2	1.29 ± 0.06
486 ± 12	38.8 ± 4.7	505 ± 12	48.8 ± 7.3	524 ± 12	80.4 ± 9.4	523 ± 8	175.0 ± 20.4	135.4 ± 15.9	1.31 ± 0.08
519 ± 10	35.8 ± 4.4	539 ± 12	56.6 ± 8.2	560 ± 12	78.7 ± 8.6	557 ± 8	156.6 ± 17.2	132.4 ± 14.6	1.29 ± 0.11
551 ± 10	33.4 ± 4.1	573 ± 12	41.2 ± 6.5	595 ± 12	84.2 ± 9.2	591 ± 8	165.7 ± 18.1	138.3 ± 15.2	1.21 ± 0.08

TABLE I: The double-differential cross sections for  $K^+$  production measured in  $pd$  collisions over the interval  $\vartheta < 4^\circ$  as a function of the kaon momentum  $p$  at four beam energies. At 2.650 GeV the differential cross sections on hydrogen are also presented, as are the  $pd/pp$  ratios. The errors do not include the overall systematic uncertainty associated with the normalizations.

Since the  $pp$  and  $pd$  data at 2.650 GeV were collected under identical conditions, many of the factors in Eq. (1) cancel out and the ratio of the cross sections for  $K^+$  production on the deuteron and proton may then be written as

$$d\sigma_{pd}^{K^+}/d\sigma_{pp}^{K^+} = (N_{pd}^{K^+}/N_{pp}^{K^+}) \times (L_{pp}^{\text{tot}}/L_{pd}^{\text{tot}}). \quad (3)$$

Numerical values for the ratio at this energy are also presented in Table I.

$T_p$ GeV	$d\sigma_{pd}^{K^+}/d\sigma_{pp}^{K^+}$	$\Delta_{\text{aver}}$	$\Delta_{\text{syst}}$
1.826	1.28	0.03	0.28
1.920	1.38	0.06	0.30
2.020	1.65	0.10	0.36
2.650	1.34	0.04	0.23

TABLE II: The mean ratio of the double-differential cross sections for  $K^+$  production in  $pd$  and  $pp$  collisions at four beam energies. The errors arising from averaging over the kaon momentum ( $\Delta_{\text{aver}}$ ) and the normalization uncertainty ( $\Delta_{\text{norm}}$ ) are also presented. The relative normalization uncertainty between the ratios measured at 1.826, 1.920, and 2.020 GeV is estimated to be 9%.

The momentum dependence of the ratio  $d\sigma_{pd}^{K^+}/d\sigma_{pp}^{K^+}$  is relatively weak at all four energies. Therefore, for comparison to the model discussed in Sec. IV, we calculate the weighted average of the ratio of the differential cross sections over the  $K^+$  momentum range. The numerical values of the ratio are given in Table II and presented graphically in Fig. 4. The averaging error  $\Delta_{\text{aver}}$  given in the table takes into account, not only the errors for

individual points, but also the momentum dependence of the ratio.

#### IV. THREE-CHANNEL MODEL

There is very little information on the production of  $K^+$  in association with excited hyperons and almost nothing on reactions where an extra pion is produced. As a consequence, we model the data purely in terms of  $K^+p\Lambda$ ,  $K^+p\Sigma^0$ , and  $K^+n\Sigma^+$  final states, though this will clearly be insufficient at the highest energy. Kaon production on a proton is assumed to be the sum of contributions from these three channels. In the estimation of the  $\Lambda$  contribution, the phase space was modified by the  $p\Lambda$  final state interaction and the  $N^*(1650)$  resonance, as suggested in Ref. [11]. On the other hand, simple phase space descriptions were used for the two  $\Sigma$  channels. The predictions were normalized to the parameterizations of the total cross sections for  $\Lambda$  and  $\Sigma$  production [17]. For this purpose, the total cross section for  $\Sigma^+$  production was assumed to be a factor 0.7 smaller than that for  $\Sigma^0$  at the same excess energy [15].

The  $pp$  calculations describe reasonably well the experimental  $K^+$  momentum spectra at the three lower energies presented in Fig. 3. However, many more channels are open at 2.65 GeV and it is not surprising that there is then a discrepancy of up to a factor of three.

Data collected on a deuterium target are also presented in Fig. 3. In this case the predictions of the three-channel model for  $K^+$  production in  $pp$  interaction have been smeared over the Fermi momentum, using the deuteron wave function derived from the Bonn potential [41]. The

Glauber shadowing effect, which was discussed in detail for the  $pd \rightarrow \eta X$  case, is included by scaling the predictions for the sum of the cross sections on the proton and neutron by a factor of 0.95 [42]. Any uncertainty in the size of this factor is small compared to the experimental errors. Note that the other effect discussed there, of  $\eta$  conversion on the second nucleon, has no parallel for  $K^+$  production.

## V. DISCUSSION

The ratio  $d\sigma_{pd}^{K^+}/d\sigma_{pp}^{K^+}$  averaged over the  $K^+$  momentum is shown in Fig. 4 for the four beam energies investigated. It can be seen from the thresholds that are indicated for the production of different strange baryonic states that, unlike for the three lower energies, at 2.65 GeV there are far more open channels than we have considered in our model. The predictions of the model for the ratio of the Fermi-smeared  $pp \rightarrow K^+p\Lambda$  plus the  $pp \rightarrow K^+N\Sigma$  total cross sections divided by the free hydrogen data are shown by the curve  $R = 1$ . Scaling this by a factor of 1.5 gives results that are in reasonable accord with the data. Simulations were also performed for the ratio of differential cross sections shown in Fig. 3 over the proton beam energy range  $T_p = 1.8 - 2.65$  GeV, where the dependence on kaon momentum is quite weak. It is seen from Fig. 4 that it makes very little difference in the modeling whether one estimates the ratios of differential or total cross sections. This gives us confidence to conclude that, despite relatively small acceptance of ANKE, the observed ratio of differential cross sections allows us to extract information on the difference between  $K^+$  production on the proton and neutron. This is especially true for the lower three energies, where the three-channel model should be effective.

The ratio results presented here clearly indicate that inclusive  $K^+$  production on the neutron is less than on the proton at all the four energies investigated. The best agreement between experimental data and our model is obtained if the ratio of the total cross sections for  $K^+$  production in the two targets has a value of  $\sigma_{pd}^{K^+}/\sigma_{pp}^{K^+} = 1.4 \pm 0.2$  which, after taking the shadowing into account, means that the ratio for  $K^+$  production in  $pn$  and  $pp$  collisions

$$\sigma_{pn}^{K^+}/\sigma_{pp}^{K^+} = 0.5 \pm 0.2. \quad (4)$$

Although the ratio seems to depend only weakly upon the beam energy, it should be noted that many different hyperons can be produced at 2.65 GeV and this can change the physics significantly.

At low energies,  $\Lambda$  production dominates the inclusive cross section and extra constraints then follow from isospin invariance. Even if the  $I = 0$  amplitude in the  $pn \rightarrow K^+n\Lambda$  reaction vanishes, there would still be the contribution from the  $I = 1$  term, so that

$$\sigma^{\text{tot}}(pn \rightarrow K^+n\Lambda)/\sigma^{\text{tot}}(pp \rightarrow K^+p\Lambda) > 1/4. \quad (5)$$

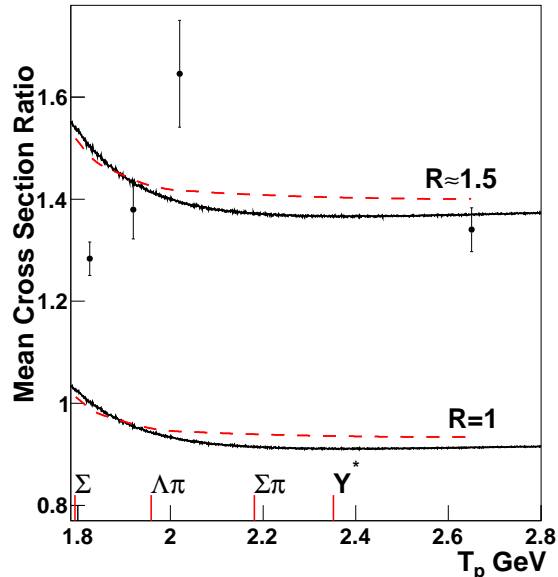


FIG. 4: (Color online) Ratio of  $K^+$  production cross sections on deuterium to hydrogen, averaged over the kaon momentum range shown in Fig. 3. Errors due to the overall normalizations are not included in the error bars. The black solid line marked  $R = 1$  represents the ratio of Fermi-smeared  $pp \rightarrow K^+p\Lambda$  plus  $pp \rightarrow K^+N\Sigma$  total cross sections divided by the free hydrogen data. The red dashed line represents the same ratio but evaluated from the differential spectra. The  $R = 1.5$  lines are simply 1.5 times these values. The parameterizations of Ref. [17], together with the newer  $\Sigma^+$  production data [14, 15], were used in these estimations. In addition to the thresholds indicated, kaon-pair production becomes possible at about 2.5 GeV.

This inequality is only exact for the total cross sections where there can be no interference between the  $I = 0$  and  $I = 1$  waves. It is not rigorous when there is a cut on the  $K^+$  momentum and especially on its angle which could, *in principle*, lead to some destructive interference over the acceptance of the ANKE spectrometer. If this possibility is neglected and only  $\Lambda$  production considered, Eq. (4) implies that

$$\sigma^{I=0}(NN \rightarrow K^+N\Lambda)/\sigma^{I=1}(NN \rightarrow K^+N\Lambda) = 1.0 \pm 0.8. \quad (6)$$

The difference between this and the result of Eq. (4) arises from the fact that, for a neutron target, half of the signal would be associated with  $K^0$  production.

The isospin ratio is much less than that determined for  $\eta$  production, where a value of about twelve has been reported near threshold [43]. It should therefore provide valuable guidance for the modeling of kaon production in nucleon-nucleon collisions as well as for experiments involving nuclear beams and/or targets.

## VI. CONCLUSIONS

The double-differential cross sections for  $K^+$  production have been measured at four different proton beam energies using hydrogen and deuterium targets. A value of  $d\sigma_{pd}^{K^+}/d\sigma_{pp}^{K^+} \approx 1.4$  has been extracted for the cross section ratio. This result is not incompatible with the  $\sigma(d\text{NaF} \rightarrow KX)/\sigma(p\text{NaF} \rightarrow KX) = 1.3 \pm 0.2$  obtained at 2.1 GeV per nucleon, though with the rather complicated NaF target [26]. In our case the ratio seems to depend weakly upon the proton beam energy and an average value of  $\sigma_{pn}^{K^+}/\sigma_{pp}^{K^+} = 0.5 \pm 0.2$  was extracted from the experimental data using a three-channel model. Taking into account the unobserved  $K^0$  production, this shows that strangeness production near threshold is rather similar for the two isospin channels of the initial nucleon-nucleon system.

To reduce the uncertainty in the cross section ratio it would be necessary to measure the spectator proton

$p_{\text{sp}}$  in the  $pd \rightarrow p_{\text{sp}}K^+n\Lambda$  reaction to ensure that the production had taken place on the neutron. This is possible at ANKE through the use of the silicon tracking telescopes and results will eventually be available on inclusive  $K^+$  production in the low energy region [23]. Alternatively, the detection of all the fast final particles in the  $pd \rightarrow p_{\text{sp}}K^0p\Lambda$  reaction would allow the kinematics of spectator proton to be reconstructed [24].

## Acknowledgments

We wish to thank the COSY machine crew and other members of the ANKE collaboration for their help during the preparation and running of the experiments reported here. This work has been partially supported by BMBF, DFG(436 RUS 113/768), Russian Academy of Science, and COSY FFE.

- 
- [1] M. Büscher *et al.*, Eur. Phys. J. A **22**, 301 (2004).
  - [2] X. Lopez *et al.*, Phys. Rev. C **75**, 011901(R) (2007).
  - [3] Z. Rudy *et al.*, Eur. Phys. J. A **23**, 379 (2005).
  - [4] S. Gautam *et al.*, J. Phys. G **37**, 085102 (2010).
  - [5] K. Tsushima, A. Sibirtsev, A. W. Thomas and G. Q. Li, Phys. Rev. C **59**, 369 (1999).
  - [6] C. Hartnack, nucl-th/0507002 (2005).
  - [7] J. T. Balewski *et al.*, Phys. Lett. B **388**, 859 (1996); Phys. Lett. B **420**, 211 (1998); Eur. Phys. J. A **2**, 99 (1998).
  - [8] R. Bilger *et al.*, Phys. Lett. B **420**, 217 (1998).
  - [9] S. Sewerin *et al.*, Phys. Rev. Lett. **83**, 682 (1999).
  - [10] P. Kowina *et al.*, Eur. Phys. J. A **22**, 293 (2004).
  - [11] M. Abdel-Bary *et al.*, Phys. Lett. B **632**, 27 (2006); M. Abdel-Bary *et al.*, Phys. Lett. B **688**, 142 (2010).
  - [12] R. I. Loutitt *et al.*, Phys. Rev. **123**, 1465 (1961).
  - [13] A. Baldini, V. Flamino, W. G. Moorhead, and D. R. O. Morison, Landolt-Börnstein, New Series, Ed. H. Schopper (Springer-Verlag, Berlin, 1988).
  - [14] Yu. Valdau *et al.*, Phys. Lett. B **652**, 27 (2007).
  - [15] Yu. Valdau *et al.*, Phys. Rev. C **81**, 045208 (2010).
  - [16] M. Abdel-Bary *et al.*, Eur. Phys. J. A **46**, 27 (2010).
  - [17] A. Sibirtsev, J. Haidenbauer, H.-W. Hammer and S. Krewald, Eur. Phys. J. A **27**, 269 (2006).
  - [18] T. Rožek *et al.*, Phys. Lett. B **643**, 251 (2006).
  - [19] M. Abdel-Bary *et al.*, Phys. Lett. B **595**, 127 (2004).
  - [20] M. Abdel-Bary *et al.*, Phys. Lett. B **649**, 252 (2007).
  - [21] R. E. Ansorge, J. A. Charlesworth, N. Intizar, W. W. Neale, and J. G. Rushbrooke, Nucl. Phys. B **60**, 157 (1973); R. E. Ansorge, J. R. Carter, J. A. Charlesworth, W. W. Neale, and J. G. Rushbrooke, Phys. Rev. D **10**, 32 (1974).
  - [22] E. Shikov, Diploma thesis, St. Petersburg University (2009).
  - [23] A. Dzyuba *et al.*, COSY proposal #203 (2010).
  - [24] M. Krapp *et al.*, IKP-Jülich Annual Report (2009).
  - [25] D. Berkley and G. B. Collins, Phys. Rev. **112**, 614 (1958).
  - [26] S. Schnetzer *et al.*, Phys. Rev. C **40**, 640 (1989).
  - [27] M. Debowski *et al.*, Z. Phys. A **356**, 313 (1996).
  - [28] S. Abd El-Samad *et al.*, Phys. Lett. B **688**, 142 (2010).
  - [29] F. Balestra *et al.*, Phys. Rev. Lett. **83**, 1534 (1999).
  - [30] G. Fäldt and C. Wilkin, Eur. Phys. J. A **24**, 431 (2005).
  - [31] A. N. Ivanov *et al.*, nucl-th/0509055.
  - [32] R. Maier *et al.*, Nucl. Instrum. Methods Phys. Res. A **390**, 1 (1997).
  - [33] A. Khoukaz *et al.*, Eur. Phys. J. D **5**, 275 (1999).
  - [34] S. Barsov *et al.*, Nucl. Instrum. Methods Phys. Res. A **462**, 354 (2001).
  - [35] M. Büscher *et al.*, Nucl. Instrum. Methods Phys. Res. A **481**, 378 (2002).
  - [36] S. Dymov *et al.*, Part. Nucl. Lett. **2**, 40 (2004).
  - [37] Yu. Uzikov, ANKE note #2 (2001).
  - [38] S. Yaschenko *et al.*, ANKE note #7 (2002).
  - [39] I. Lehmann *et al.*, Nucl. Instrum. Methods Phys. Res. A **530**, 275 (2004).
  - [40] S. Barsov *et al.*, Eur. Phys. A **21**, 521 (2004).
  - [41] R. Machleidt, K. Holinde, and Ch. Elster, Phys. Rep. **149**, 1 (1987).
  - [42] E. Chiaivassa *et al.*, Phys. Lett. B **337**, 192 (1994).
  - [43] H. Calén, *et al.*, Phys. Rev. Lett. **79**, 2642 (1997).